Comptes Rendus

Chimie

Nesrine Hafedh, Basim H. Asghar and Faouzi Aloui

Novel functional [4]helicenes through a photooxidation pathway. Investigation of the absorption and fluorescence in solution

Full paper / *Article*

Novel functional [4]helicenes through a photooxidation pathway. Investigation of the absorption and fluorescence in solution

Nouveaux [4]hélicènes par voie de photooxydation. Investigation de l'absorption et de la fluorescence en solution

Nesrine Hafedh [a], **Basim H. Asghar** [b] **and Faouzi Aloui** *[*, a]

[a] University of Monastir, Faculty of Sciences, Laboratory of Asymmetric Synthesis and Molecular Engineering of Materials for Organic Electronics (LR18ES19), Avenue of Environment 5019 Monastir, Tunisia

[b] Department of Chemistry, Faculty of Applied Science, Umm Al-Qura University, Makkah, Saudi Arabia

E-mails: hafedh.nessrine23@gmail.com (N. Hafedh), bhasghar@uqu.edu.sa
(B. H. Asghar), alouifaouzi0@gmail.com (F. Aloui)

Abstract. Novel functional [4]helicenes have been designed and synthesized, in 54%–72% overall yields, through an operational and simple two-step photochemical approach starting from various *p*-substituted phenylacetonitriles, and were characterized by NMR (^{1}H, ^{13}C, and COSY) and FT-IR spectroscopies. UV–Vis absorption properties of these tetracyclic π-conjugated systems have been experimentally investigated in various solvents and their optical gap energy was estimated to be less than 3.28 eV. The photoluminescence properties of these molecules have been evaluated in solutions and an emission in the blue region of the visible spectrum was noted. The obtained results seem encouraging for the examination of such compounds as promising materials for optoelectronic applications.

Résumé. De nouveaux [4]hélicènes fonctionnels ont été conçus et synthétisés, avec des rendements globaux de 54%–72%, selon une approche photochimique opérationnelle et simple en deux étapes à partir de divers phénylacétonitriles *p*-substitués et ont été caractérisés par RMN (^{1}H, ^{13}C et COSY) et IR à transformée de Fourier. Les propriétés d'absorption UV–Vis de ces systèmes tétracycliques conjugués ont été étudiées expérimentalement dans divers solvants et leur énergie de gap optique a été estimée à moins de 3.28 eV. Les propriétés de photoluminescence de ces molécules ont été évaluées en solution et une émission a été notée dans la région bleue du spectre visible. Les résultats obtenus semblent encourageants pour l'examen de tels composés en tant que matériaux prometteurs pour des applications optoélectroniques.

* Corresponding author.

1. Introduction

[4]Helicenes, called benzo[*c*]phenanthrenes, are organic molecules consisting of four *ortho*-fused benzene rings and belong to the class of polycyclic aromatic hydrocarbons (PAHs). These smallest helicenes have attracted considerable attention in view of their π-conjugated system and their twisted geometry.

The helicity of the benzo[*c*]phenanthrene (B[*c*]p) can be further reinforced through bulky substitution at 1 and 12 positions (Figure 1) of the terminal rings [1], which makes the molecule configurationally stable and can be resolved to give *P*- and *M*-enantiomers [2]. As a first example of chiral tetracyclic skeleton, Newman and co-workers [3] reported the synthesis and an optical resolution leading to the [4]helicene derivative **1**. Since then, some [4]helicene derivatives have been synthesized in optically active form; for example, the lactone-type **2** [4]. Moroever, Carreño and co-workers have developed an enantioslective approach leading to the [4]helicene quinone **3** [5]. In an independent study, the [4]helicenium cation **4** was described as a chiral analog of hetero[4]helicenes [6]. This charged compound obtained after resolution has demonstrated a high configurational stability. More recently, we have reported the synthesis of the nitrile-grafted benzo[*c*]phenanthrene derivatives **5a–b** and used them to achieve enantiopure [6]helicenes [7,8].

[4]Helicenes have shown various applications in different areas thanks to their particular structure and their interesting properties. They were exploited in catalysis [9,10], supramolecular assemblies [11], molecular recognition [12], and charge transfer complexation [13] and as motors [14]. Incorporation of heteroatoms into the [4]helicene skeleton has considerably amplified its electronic and photophysical properties, thus allowing its application in electronic devices [15–28]. For example, the phosphorus- and boron-doped [4]helicenes **6** and **7** (Figure 2) have shown a strong green fluorescence with quantum yields of 0.83 and 0.81, respectively [29,30]. Organometallic helicenes are also regarded as strong chiral emitters [31–35]. Among these conjugated systems, a cycloplatinated [6]helicene [36] has been prepared from the [4]helicene derivative **8**, which reveals original electronic, chiroptical, and photophysical properties.

These studies have inspired us to design and develop new [4]helicene derivatives bearing reactive functional groups by incorporating sulfur into their skeleton to evaluate their photophysical properties experimentally. Our synthetic strategy is based on the preparation of valuable α, β-unsaturated nitriles which were subjected to UV irradiation giving rise to the target [4]helicenes.

2. Experimental section

2.1. *General methods*

Unless otherwise noted, reagents and solvents used in this work were purchased from Sigma–Aldrich. All reactions were carried out under an argon atmosphere and were monitored by thin-layer chromatography (TLC) using commercial silica-gel plate 60 coated with a fluorescence indicator (SiliCycle Chemical division, 0.25 mm, F254). The use of UV light at 254 nm or 365 nm allowed visualization of the TLC plate. Organic compounds were purified using silica gel obtained from SiliCycle Chemical division (40–63 nm; 230–240 mesh). All mixed solvent eluents are reported as v/v solutions. Melting points were measured on a Bibby Scientific Stuart Digital, Advanced, SMP30. ^{1}H and ^{13}C spectra were taken on a Bruker AC 300 instrument in CDCl$_3$ (300 MHz (^{1}H) and 75 MHz (^{13}C)). Signals due to the solvent served as the internal standard (CHCl$_3$: δ 7.26 for ^{1}H, δ 77.16 for ^{13}C). Chemical shifts (δ) are reported in parts per million (ppm) relative to TMS. Coupling constant *J* is given in Hz. Photochemical reactions were performed using a falling-film photoreactor and a high-pressure Hg-vapor lamp (500 W, Helios Italquartz). UV–Vis spectra were recorded on a spectrophotometer UV-1600PC, using quartz cuvettes of 1 cm path length. Steady-state luminescence spectra were measured using a Jobin Yvon FluoroMax-2
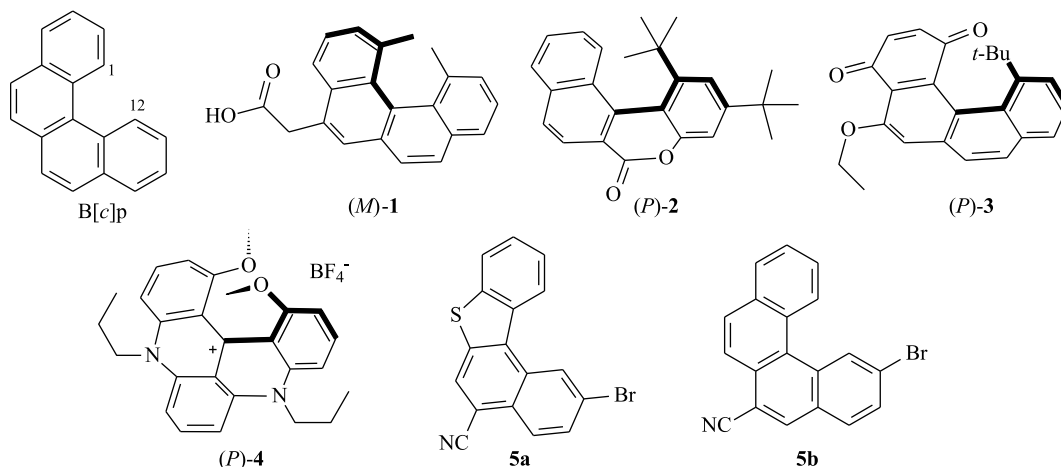
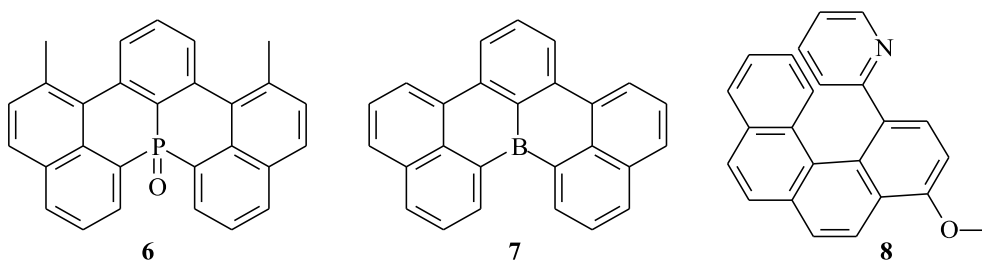**Figure 1.** Representative examples of [4]Helicene derivatives.

Figure 2. [4]Helicene derivatives as emitters.

spectrofluorometer, fitted with a red-sensitive Hamamatsu R928 photomultiplier tube. Samples for emission measurements were contained within quartz cuvettes of 1 cm path length.

2.2. *General procedure for the preparation of the* α, β*-unsaturated nitriles* **9a–h**

1 molar equivalent of *p*-substituted phenylacetonitrile was mixed with 1 molar equivalent of 2-naphtaldehyde or benzo[*b*]thiophene-2-carbaldehyde in dry methanol (30 mL) and the solution was stirred at 0 °C for 10 minutes. Then, 2 molar equivalents of sodium methoxide was added in small portions and the mixture was stirred for 30 minutes at 0 °C, and then for 4 hours at room temperature. The precipitate was filtered, washed with cold methanol followed by water, and dried in air.

2.2.1. *(Z)-2-(naphthalen-2-yl)-3-phenylacrylonitrile (9a)*

Yellow solid, 81%, m.p = 117–119 °C; ^{1}H NMR (300 MHz, CDCl$_3$): δ (ppm) : 7.40–7.54 (m, 3H), 7.52–7.60 (m, 2H), 7.70 (s, 1H), 7.73–7.77 (m, 2H), 7.87–7.95 (m, 3H), 8.09 (d, *J* = 8.7 Hz, 1H), 8.32 (s, 1H, H$_{vinyl}$); ^{13}C NMR (75 MHz, CDCl$_3$): δ (ppm): 111.3 (C), 117.5 (CN), 124.8 (CH), 125.5 (2CH), 126.2 (CH), 127.0 (CH), 127.2 (CH), 128.1 (CH), 128.2 (CH), 128.5 (2CH), 128.6 (CH), 129.8 (CH), 130.8 (C), 132.6 (C), 133.6 (C), 134.2 (C), 141.6 (CH); HRMS (MALDI-TOF) Cald. For (C$_{19}$H$_{13}$NNa) [M+Na]$^+$: 278.0945. Found: 278.0941; Anal. Calcd for C$_{19}$H$_{13}$N: C, 89.38; H, 5.13. Found: C, 89.32; H, 5.11.

2.2.2. *(Z)-2-(4-methylphenyl)-3-(naphthalen-2-yl)acrylonitrile (9b)*

White solid, 81%, m.p = 128–130 °C; ^{1}H NMR (300 MHz, CDCl$_3$): δ (ppm): 2.41 (s, 3H, CH$_3$), 7.26

(d, J = 8.1 Hz, 2H), 7.50–7.57 (m, 2H), 7.61–7.64 (m, 3H), 7.84–7.92 (m, 3H), 8.05 (d, J = 8.7 Hz, 1H), 8.28 (s, 1H, H_{vinyl}); ^{13}C NMR (75 MHz, CDCl$_3$): δ (ppm): 20.6 (CH$_3$), 111.3 (C), 117.6 (CN), 124.8 (CH), 125.4 (2CH), 126.2 (CH), 126.9 (CH), 127.2 (CH), 128.1 (CH), 128.2 (CH), 129.2 (2CH), 129.6 (CH), 130.9 (C), 131.4 (C), 132.7 (C), 133.5 (C), 138.8 (C), 140.5 (CH); HRMS (MALDI-TOF) Cald. For (C$_{20}$H$_{15}$NNa) [M+Na]$^+$: 292.1102. Found: 292.1098; Anal. Calcd for C$_{20}$H$_{15}$N: C, 89.19; H, 5.61. Found: C, 89.11; H, 5.59.

2.2.3. *(Z)-2-(4-fluorophenyl)-3-(naphthalen-2-yl)acrylonitrile (9c)*

White solid, 73%, m.p = 148–150 °C; ^{1}H NMR (300 MHz, CDCl$_3$): δ (ppm): 7.18 (t, J = 8.4 Hz, 2H), 7.54–7.59 (m, 2H), 7.63 (s, 1H), 7.69–7.74 (m, 2H), 7.87–7.95 (m, 3H), 8.07 (d, J = 8.4 Hz, 1H), 8.30 (s, 1H, H_{vinyl}); ^{13}C NMR (75 MHz, CDCl$_3$): δ (ppm): 110.2 (C), 115.4 (d, J_{C-F} = 21.9 Hz, 2CH), 117.4 (CN), 124.6 (CH), 126.3 (CH), 127.1 (CH), 127.2 (CH), 127.3 (CH), 127.4 (CH), 128.2 (2CH), 129.8 (CH), 130.3 (C), 130.6 (C), 132.6 (C), 133.7 (C), 141.5 (CH), 161.1 (d, J_{C-F} = 248 Hz, C–F).; ^{19}F NMR, 282 MHz, CDCl$_3$): δ (ppm): −108.84; HRMS (MALDI-TOF) Cald. For (C$_{19}$H$_{12}$FNNa) [M+Na]$^+$: 296.0851. Found: 296.0847; Anal. Calcd for C$_{19}$H$_{12}$FN: C 83.50; H 4.43. Found: C 83.40; H 4.45.

2.2.4. *(Z)-2-(4-chlorophenyl)-3-(naphthalen-2-yl)acrylonitrile (9d)*

White solid, 80%, m.p = 167–169 °C; ^{1}H NMR (300 MHz, CDCl$_3$): δ (ppm): 7.43 (d, J = 8.4 Hz, 2H), 7.53–7.60 (m, 2H), 7.65–7.68 (m, 3H), 7.87–7.95 (m, 3H), 8.08 (dd, J_1 = 1.5 Hz, J_2 = 7.5 Hz, 1H), 8.31 (s, 1H, H_{vinyl}); ^{13}C NMR (75 MHz, CDCl$_3$): δ (ppm): 110.6 (C), 117.7 (CN), 125.1 (CH), 126.8 (CH), 127.2 (2CH), 127.7 (2CH), 128.7 (2CH), 129.2 (2CH); 130.5 (CH), 131.0 (C), 133.1 (C), 133.2 (C), 134.2 (C), 135.2 (C), 142.4 (CH); HRMS (MALDI-TOF) Cald. For (C$_{19}$H$_{12}$ClNNa) [M+Na]$^+$: 312.0555. Found: 312.0551; Anal. Calcd for C$_{19}$H$_{12}$ClN: C 78.76; H 4.17. Found: C 78.81; H 4.11.

2.2.5. *(Z)-3-(benzo[b]thiophen-2-yl)-2-phenylacrylonitrile (9e)*

Yellow solid, 87%, m.p = 128–130 °C; ^{1}H NMR (300 MHz, CDCl$_3$) : δ (ppm): 7.37–7.48 (m, 5H), 7.68–7.71 (m, 3H), 7.81–7.87 (m, 3H); ^{13}C NMR (75 MHz, CDCl$_3$): δ (ppm): 110.4 (C), 117.2 (CN), 121.9 (CH), 124.0 (CH), 124.5 (CH), 125.4 (2CH), 125.9 (CH), 128.6

(2CH), 128.8 (CH), 129.0 (CH), 133.4 (C), 134.0 (CH), 137.1 (C), 138.2 (C), 140.6 (C); HRMS (MALDI-TOF) Cald. For (C$_{17}$H$_{11}$NSNa) [M+Na]$^+$: 284.0509. Found: 284.0505; Anal. Calcd for C$_{17}$H$_{11}$NS: C 78.13; H 4.24. Found: C 78.03; H 4.31.

2.2.6. *(Z)-3-(benzo[b]thiophen-2-yl)-2-(p-tolyl)acrylonitrile (9f)*

Yellow solid, 90%, m.p = 158–160 °C; ^{1}H NMR (300 MHz, CDCl$_3$): δ (ppm): 2.40 (s, 3H, CH$_3$), 7.24 (d, J = 8.1 Hz, 2H), 7.36–7.43 (m, 2H), 7.56 (d, J = 8.1 Hz, 2H), 7.66 (s, 1H, H_{vinyl}), 7.81–7.86 (m, 3H); ^{13}C NMR (75 MHz, CDCl$_3$): δ (ppm): 20.6 (CH$_3$), 110.4 (C), 117.3 (CN), 121.8 (CH), 123.9 (CH), 124.4 (CH), 125.3 (2CH), 125.8 (CH), 128.5 (CH), 129.3 (2CH), 130.6 (C), 133.0 (CH), 137.3 (C); 138.3 (C), 139.1 (C), 140.5 (C); HRMS (MALDI-TOF) Cald. For (C$_{18}$H$_{13}$NSNa) [M+Na]$^+$: 298.0666. Found: 298.0662; Anal. Calcd for C$_{18}$H$_{13}$NS: C 78.51; H 4.76. Found: C 78.63; H 4.81.

2.2.7. *(Z)-3-(benzo[b]thiophen-2-yl)-2-(p-fluorophenyl)acrylonitrile (9g)*

Yellow solid, 79%, m.p = 178–180 °C; ^{1}H NMR (300 MHz, CDCl$_3$): δ (ppm): 7.11–7.16 (m, 2H), 7.37–7.45 (m, 2H), 7.62–7.67 (m, 3H), 7.80–7.86 (m, 3H); ^{13}C NMR (75 MHz, CDCl$_3$): δ (ppm): 109.0 (C), 115.6 (d, J_{C-F} = 22 Hz, 2CH), 117.2 (CN), 121.9 (CH), 124.1 (CH), 124.6 (CH), 126.1 (CH), 127.2 (d, J_{F-C} = 8.2 Hz, CH), 129.3 (d, J_{F-C} = 8 Hz, CH), 129.5 (C), 134.04 (CH), 134.07 (CH), 136.9 (C), 138.1 (C), 140.5 (C), 161.1 (d, J_{F-C} = 249.2 Hz, C–F); ^{19}F NMR, 282 MHz, CDCl$_3$): δ (ppm): −111.18; HRMS (MALDI-TOF) Cald. For (C$_{17}$H$_{10}$FNSNa) [M+Na]$^+$: 302.0415. Found: 302.0411; Anal. Calcd for C$_{17}$H$_{10}$FNS: C 73.10; H 3.61. Found: C 73.03; H 3.58.

2.2.8. *(Z)-3-(benzo[b]thiophen-2-yl)-2-(p-chlorophenyl)acrylonitrile (9h)*

Yellow solid, 72%, m.p = 203–205 °C; ^{1}H NMR (300 MHz, CDCl$_3$): δ (ppm): 7.40–7.44 (m, 2H), 7.44–7.47 (m, 2H), 7.60 (d, J = 6.9 Hz, 2H), 7.70 (s, 1H), 7.83–7.88 (m, 3H); ^{13}C NMR (75 MHz, CDCl$_3$): δ (ppm): 109.0 (C), 116.9 (CN), 121.9 (CH), 124.1 (CH), 124.6 (CH), 126.1 (CH), 126.5 (2CH), 128.8 (2CH), 129.5 (CH), 131.8 (C), 134.3 (CH), 134.9 (C), 136.8 (C), 138.1 (C), 140.7 (C); HRMS (MALDI-TOF) Cald. For (C$_{17}$H$_{10}$ClNSNa) [M+Na]$^+$: 318.0120. Found: 318.0116; Anal. Calcd for C$_{17}$H$_{10}$ClNS: C 69.03; H 3.41. Found: C 69.07; H 3.44.

2.3. General procedure for the photocyclization reaction

1-liter solution of toluene containing 600 mg of α, β-unsaturated nitrile **9** and 1.1 molar equivalents of iodine was degassed for 10–15 minutes. Then, 50 molar equivalents of propylene oxide were added and the mixture was irradiated for 2–3 hours using a falling-film photoreactor and a high-pressure Hg-vapor lamp (500 W, Helios Italquartz). After completion of the reaction (TLC), the solvent was removed under reduced pressure and the crude residue was purified by silica-gel column chromatography with cyclohexane/EtOAc (80:20) as the eluent. Spectroscopic data of [4]helicene derivatives are given subsequently.

2.3.1. Benzo[c]phenanthrene-5-carbonitrile (10a)

Yellow solid, 71%, m.p = 125–127 °C; ^{1}H NMR (300 MHz, CDCl$_3$): δ (ppm): 7.72–7.75 (m, 2H, H$_{9,11}$), 7.78–7.81 (m, 3H, H$_{2,3,7 or 8}$), 7.95 (d, J = 8.4 Hz, 1H, H$_8$ or H$_7$), 8.04–8.07 (m, 1H, H$_{10}$), 8.29 (s, 1H, H$_6$), 8.44–8.49 (m, 1H, H$_4$), 9.05–9.08 (m, 1H, H$_{12}$), 9.11–9.14 (m, 1H, H$_1$); ^{13}C NMR (75 MHz, CDCl$_3$): δ (ppm): 108.8 (C), 117.2 (CN), 125.3 (CH), 125.5 (CH), 126.3 (CH), 126.9 (CH), 127.0 (CH), 127.1 (CH), 127.8 (CH), 127.9 (CH), 128.1 (CH), 128.2 (CH), 128.5 (C), 129.0 (C), 129.5 (C), 129.8 (C), 130.3 (C), 134.0 (CH), 134.2 (C); HRMS (MALDI-TOF) Cald. For (C$_{19}$H$_{11}$N) [M]$^+$: 253.0891. Found: 253.0887; Anal. Calcd for C$_{19}$H$_{11}$N: C 90.09, H 4.38. Found: C 90.17, H 4.41; FT-IR: ν (cm^{-1}): 534, 567, 607, 662, 735, 807, 903, 1063, 1160, 1240, 1367, 1424, 1496, 1592, 1728, 1929, 2210, 3059.

2.3.2. 2-Methylbenzo[c]phenanthrene-5-carbonitrile (10b)

Yellow solid, 81%, m.p = 185–187 °C; ^{1}H NMR (300 MHz, CDCl$_3$): δ (ppm): 2.68 (s, 3H, CH$_3$), 7.64 (d, J = 8.1 Hz, 1H, H$_3$), 7.71–7.78 (m, 3H, H$_{9,11,7 or 8}$), 7.92 (d, J = 8.7 Hz, 1H, H$_8$ or H$_7$), 8.03–8.06 (m, 1H, H$_{10}$), 8.20 (s, 1H, H$_6$), 8.32 (d, J = 8.1 Hz, 1H, H$_4$), 8.90 (s, 1H, H$_1$), 9.05 (d, J = 9 Hz, 1H, H$_{12}$); ^{13}C NMR (75 MHz, CDCl$_3$): δ (ppm): 21.2 (CH$_3$), 108.6 (C), 117.4 (CN), 125.1 (CH), 125.6 (CH), 126.2 (CH), 126.7 (CH), 127.4 (CH), 127.7 (CH), 127.9 (CH), 128.1 (CH), 128.4 (C), 128.7 (C), 128.8 (CH), 129.1 (C), 129.4 (C), 129.7 (C), 133.0 (CH), 134.1 (C), 137.1 (CH); HRMS (MALDI-TOF) Cald. For (C$_{20}$H$_{13}$N) [M]$^+$: 267.1047. Found: 267.1043. Anal. Calcd for C$_{20}$H$_{13}$N: C 89.86,

H 4.90. Found: C 89.96, H 4.94; FT-IR: ν (cm^{-1}): 519, 664, 747, 811, 901, 1047, 1156, 1238, 1384, 1439, 1502, 1611, 2221, 2940, 3067.

### 2.3.3. 2-Fluorobenzo[c]phenanthrene-5-carbonitrile (10c)

Yellow solid, 82%, m.p = 225–227 °C; ^{1}H NMR (300 MHz, CDCl$_3$): δ (ppm): 7.53–7.60 (m, 1H, H$_3$), 7.74–7.82 (m, 3H, H$_{9,11,7 or 8}$), 7.98 (d, J = 8.4 Hz, 1H, H$_8$ or H$_7$), 8.06 (d, J = 8.1 Hz, 1H, H$_{10}$), 8.26 (s, 1H, H$_6$), 8.42 (dd, J_{H-H} = 9 Hz, J_{H-F} = 6 Hz, 1H, H$_4$), 8.68 (dd, J_{H-H} = 1.8 Hz, J_{H-F} = 11.7 Hz 1H, H$_1$), 8.9 (d, J = 8.1 Hz, 1H, H$_{12}$); ^{13}C NMR (101 MHz, CDCl$_3$): δ (ppm): 108.9 (C), 113.2 (d, J_{C-F} = 24.03 Hz, CH), 116.8 (d, $_{C-F}$ = 24.4 Hz, CH), 117.7 (CN), 126.0 (CH), 127.3 (CH), 127.45 (C), 127.46 (C), 127.5 (CH), 127.7 (CH), 128.1 (d, J_{C-F} = 9.1 Hz, CH), 128.9 (CH), 129.3 (CH), 129.4 (C), 129.5 (C), 131.3 (d, J_{F-C} = 8.9 Hz, C), 133.9 (CH), 134.5 (C), 160.8 (d, J_{F-C} = 248.6 Hz, C-F); ^{19}F NMR, 282 MHz, CDCl$_3$): δ (ppm): −109.6; HRMS (MALDI-TOF) Cald. For (C$_{19}$H$_{10}$NF) [M]$^+$: 271.0797. Found: 271.0793; Anal. Calcd for C$_{19}$H$_{10}$NF: C 84.12, H 3.72. Found: C 84.03, H 3.70; FT-IR: ν (cm^{-1}): 542, 647, 670, 711, 743, 807, 895, 1183, 1416, 1504, 1616, 1720, 2218, 3059.

2.3.4. 2-Chlorobenzo[c]phenanthrene-5-carbonitrile (10d)

Yellow solid, 85%, m.p = 137–139 °C; ^{1}H NMR (300 MHz, CDCl$_3$): δ (ppm): 7.61–7.69 (m, 4H, H$_{3,9,11,7 or 8}$), 7.86 (d, J = 8.7 Hz, 1H, H$_8$ or H$_7$), 7.93 (dd, J_1 = 2.4 Hz, J_2 = 7.2 Hz, 1H, H$_{10}$), 8.16 (s, 1H, H$_6$), 8.23 (d, = 8.7 Hz, 1H, H$_4$), 8.84 (d, J = 8.1 Hz, H$_{12}$), 8.96 (d, J = 1.8 Hz, 1H, H$_1$); ^{13}C NMR (75 MHz, CDCl$_3$): δ (ppm): 108.8 (C), 117.5 (CN), 125.9 (CH), 127.2 (CH), 127.4 (CH), 127.5 (CH), 127.7 (CH), 127.8 (CH), 128.1 (CH), 128.9 (CH), 129.0 (C), 129.1 (C), 129.2 (C), 129.3 (CH), 129.5 (C), 130.8 (C), 134.1 (C), 134.6 (C), 134.7 (CH); HRMS (MALDI-TOF) Cald. For (C$_{19}$H$_{10}$NCl) [M]$^+$: 287.0501. Found: 287.0497; Anal. Calcd for C$_{19}$H$_{10}$NCl: C 79.31, H 3.50. Found: C 79.41, H 3.55; FT-IR: ν(cm^{-1}): 506, 638, 677, 748, 802, 904, 1013, 1052, 1091, 1154, 1240, 1357, 1388, 1419, 1489, 1591, 1692, 2223, 3059.

2.3.5. Benzo[b]naphtho[2,1-d]thiophene-7-carbonitrile (10e)

Yellow solid, 80%, m.p = 172–174 °C; ^{1}H NMR (300 MHz, CDCl$_3$): δ (ppm): 7.51–7.67 (m, 2H, H$_{2,3}$), 7.71–
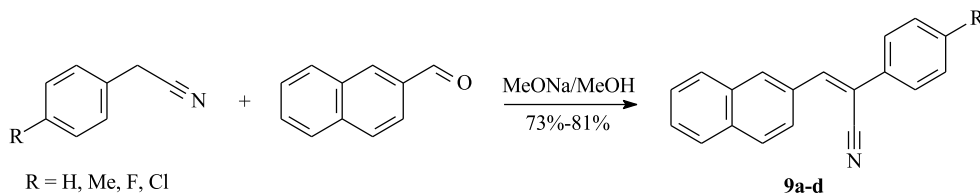
Scheme 1. Synthesis of α, β-unsaturated nitriles **9a–d** from 2-naphtaldehyde.

7.84 (m, 2H, $H_{9,10}$), 7.99 (dd, $J_1 = 2.1$ Hz, $J_2 = 7.2$ Hz, 1H, H_4), 8.27 (s, 1H, H_6), 8.38 (dd, $J_1 = 1.5$ Hz, $J_2 = 8.1$ Hz, 1H, H_8), 8.79 (dd, $J_1 = 1.8$ Hz, $J_2 = 7.5$ Hz 1H, H_1), 8.96 (d, $J = 8.1$ Hz, 1H, H_{11}); ^{13}C NMR (75 MHz, CDCl$_3$): δ (ppm): 108.7 (C), 117.1 (CN), 122.8 (CH), 123.1 (CH), 124.9 (CH), 125.0 (CH), 126.1 (CH), 126.3 (CH), 126.4 (CH), 127.4 (CH), 127.9 (CH), 129.6 (C), 129.7 (C), 132.3 (C), 135.0 (C), 136.1 (C), 140.7 (C); HRMS (MALDI-TOF) Cald. For (C$_{17}$H$_9$NS) [M]$^+$: 259.0455. Found: 259.0451; Anal. Calcd for C$_{17}$H$_9$NS: C 78.74, H 3.50. Found: C 78.65, H 3.47; FT-IR: ν (cm^{-1}): 476, 539, 610, 657, 713, 744, 775, 870, 1012, 1115, 1154, 1201, 1241, 1320, 1367, 1430, 1509, 1580, 2219.

2.3.6. *10-Methylbenzo[b]naphtho[2,1-d]thiophene-7-carbonitrile (10f)*

Yellow solid, 80%, m.p = 220–222 °C; ^{1}H NMR (300 MHz, CDCl$_3$): δ (ppm): 2.68 (s, 3H, CH$_3$), 7.52–7.65 (m, 3H, $H_{2,3,9}$), 7.97 (d, $J = 7.8$ Hz, 1H, H_4), 8.17 (s, 1H, H_6), 8.24 (d, $J = 8.4$ Hz, 1H, H_8), 8.72 (s, 1H, H_{11}), 8.77 (d, $J = 8.1$ Hz, 1H, H_1); ^{13}C NMR (75 MHz, CDCl$_3$): δ (ppm): 21.8 (CH$_3$), 108.5 (C), 117.2 (CN), 122.6 (CH), 122.8 (CH); 124.7 (CH), 124.9 (CH), 125.9 (CH), 126.1 (CH), 126.3 (CH), 127.8 (C), 128.3 (CH), 129.8 (C), 131.8 (C), 135.1 (C), 136.1 (C), 138.1 (C), 140.6 (C); HRMS (MALDI-TOF) Cald. For (C$_{18}$H$_{11}$NS) [M]$^+$: 273.0612. Found: 273.0608; Anal. Calcd for C$_{18}$H$_{11}$NS: C 79.09, H, 4.06. Found: C 79.19, H 4.01; FT-IR: ν (cm^{-1}): 542, 623, 655, 711, 751, 807, 879, 927, 1031, 1071, 1160, 1183, 1240, 1312, 1360, 1384, 1432, 1521, 1616, 1704, 2210, 2923, 3059.

2.3.7. *10-Fluorobenzo[b]naphtho[2,1-d]thiophene-7-carbonitrile (10g)*

Yellow solid, 84%, m.p = 235–237 °C; ^{1}H NMR (300 MHz, CDCl$_3$): δ (ppm): 7.53 (td, $J_1 = 2.1$ Hz, $J_2 = 8.1$ Hz, 1H, H_3), 7.60–7.71 (m, 2H, $H_{2,9}$), 8.04 (d, $J = 8.1$ Hz, 1H, H_8), 8.30 (s, 1H, H_6), 8.41 (dd, $J_{H-H} = 9$ Hz, $J_{H-F} = 5.7$ Hz, 1H, H_4), 8.62 (dd, $J_{H-H} =$ 2.4 Hz, $J_{H-F} = 11.1$ Hz, 1H, H_{11}), 8.73 (d, $J = 7.8$ Hz, 1H, H_1); ^{13}C NMR (75 MHz, CDCl$_3$): δ (ppm): 108.5 (d, $J_{F-C} = 23.3$ Hz, CH), 109.0 (C), 116.5 (d, $J_{F-C} = 24.6$ Hz, CH), 117.5 (CN), 123.5 (CH), 125.0 (CH), 125.7 (CH), 127.0 (C), 127.1 (CH), 127.2 (CH), 129.1 (d, $J_{F-C} = 9.4$ Hz, CH), 131.0 (C), 132.2 (C), 135.2 (C), 137.7 (C), 141.1 (C), 160.6 (d, $J_{F-C} = 246.6$ Hz, CF); ^{19}F NMR (282 MHz, CDCl$_3$): δ (ppm): −109.17; HRMS (MALDI-TOF) Cald. For (C$_{17}$H$_8$FNS) [M]$^+$: 277.0361. Found: 277.0357; Anal. Calcd for C$_{17}$H$_8$FNS: C 73.63, H, 2.91. Found: C 73.71, H, 2.97; ν (cm^{-1}) = 584, 630, 711, 747, 820, 892, 973, 1037, 1154, 1181, 1236, 1326, 1353, 1426, 1516, 1616, 2222, 3063.

### 2.3.8. *10-Chlorobenzo[b]naphtho[2,1-d]thiophene-7-carbonitrile (10h)*

White solid, 96%, m.p = 212–214 °C; ^{1}H NMR (300 MHz, CDCl$_3$): δ (ppm): 7.58–7.67 (m, 3H, $H_{2,3,9}$), 7.99 (d, $J = 7.5$ Hz, 1H, H_4), 8.22 (s, 1H, H_6), 8.25 (d, $J = 9$ Hz, 1H, H_8), 8.62 (d, $J = 8.4$ Hz, 1H, H_1), 8.83 (d, $J = 1.5$ Hz, 1H, H_{11}); ^{13}C NMR (75 MHz, CDCl$_3$): δ (ppm): 108.3 (C), 116.7 (CN), 122.4 (CH), 122.9 (CH), 124.5 (CH), 125.2 (CH), 126.6 (CH), 127.1 (CH), 127.43 (CH), 127.47 (CH), 127.7 (C), 129.9 (C), 131.1 (C), 134.3 (C), 134.4 (C), 137.0 (C), 140.6 (C); HRMS (MALDI-TOF) Cald. For (C$_{17}$H$_8$ClNS) [M]$^+$: 293.0065. Found: 293.0061; Anal. Calcd for C$_{17}$H$_8$ClNS: C 69.51, H 2.74. Found: C 69.62, H 2.78; FT-IR: ν (cm^{-1}): 485, 560, 609, 667, 717, 741, 783, 808, 883, 907, 948, 1089, 1130, 1155, 1238, 1312, 1354, 1429, 1611, 2222, 3058.

3. Results and discussion

In the first step, we prepared different α, β-unsaturated nitriles, as precursors for the [4]helicenes, through Knoevenagel reaction. We sought to functionalize our olefin using various *p*-substituted phenylacetonitriles, which were condensed with 2-naphtaldehyde affording nitriles **9a–d** in 73%–81%
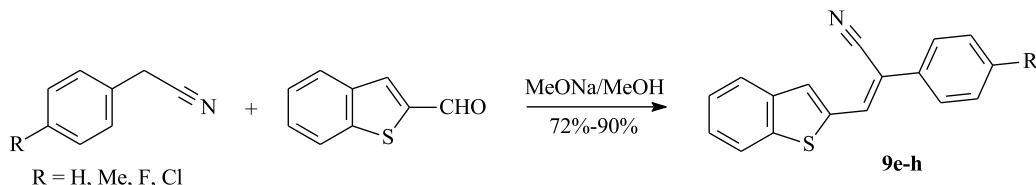
Scheme 2. Synthesis of α,β-unsaturated nitriles **9e–h** from benzo[*b*]thiophene-2-carbaldehyde.
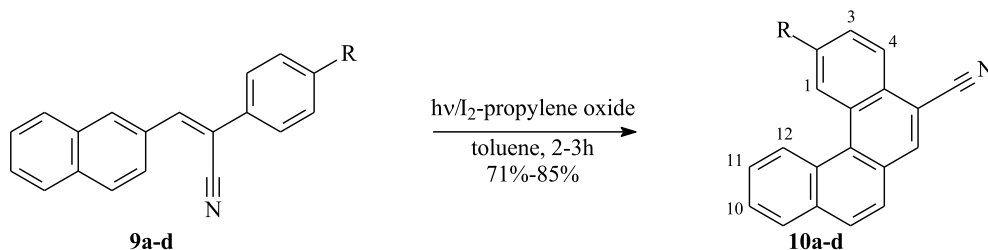
Scheme 3. Photocyclization of the α,β-unsaturated nitriles **9a–d** into [4]helicenes **10a–d**.

Table 1. Chemical yields of the α,β-unsaturated nitriles **9a–h**

α,β-unsaturated nitrile	R	Yield (%)[a]
9a	H	81
9b	Me	80
9c	F	73
9d	Cl	80
9e	H	87
9f	Me	90
9g	F	79
9h	Cl	72

[a]Isolated yields.

Table 2. Chemical yields of [4]helicenes **10e–h**

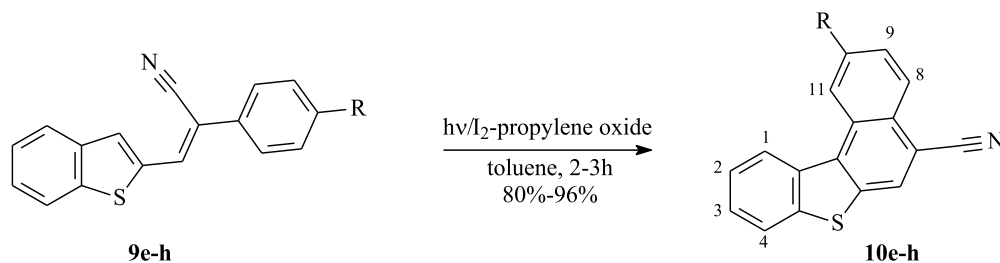| [4]helicene	R	Yield (%)[a]
10a	H	71
10b	Me	81
10c	F	82
10d	Cl	85
10e	H	80
10f	Me	80
10g	F	84
10h	Cl	96

[a]Isolated yields.

yields (Scheme 1, Table 1). A wide variety of literature conditions for the Knoevenagel condensation can be performed [37,38]. Herein, we report an economic and rapid synthesis, using sodium methoxide as a base and dry methanol as a solvent at room temperature to provide the desired diarylethenes, with *Z*-configuration, which are recovered by simple filtration.

According to the same synthetic approach, we have carried out the Knoevenagel reaction between the *p*-substituted arylacetonitriles and benzo[*b*]thiophene-2-carbaldehyde which provides a series of (hetero)functionalized α, β-unsaturated nitriles **9e–h** in 72%–90% yields (Scheme 2, Table 1).

The resulting α,β-unsaturated nitriles **9a–h** were then subjected to photocyclization providing new tetracyclic systems using an immersion 500 W Hg-vapor lamp (Scheme 3). The irradiation was carried out using 600 mg of each α,β-unsaturated nitrile in 1 L of toluene, in the presence of iodine and propylene oxide. The photocyclization reaction requires high dilution to avoid intramolecular couplings [39] or dimerization of the substrate [40]. Thus, diarylethenes **9a–d** were photoconverted into the benzo[*c*]phenanthrene-5-carbonitrile derivatives **10a–d** in 71%–85% yields (Table 2).

On the other hand, similar experimental conditions were used for the photolysis of α,β-unsaturated nitriles **9e–h**. This allows the formation

Scheme 4. Photocyclization of the α, β-unsaturated nitriles **9e–h** into [4]helicene **10e–h**.

of the expected benzo[*b*]naphto[2,1-*d*]thiophene-7-carbonitrile derivatives **10e–h** in 80%–96% yields (Scheme 4, Table 2).

The structural assignment of [4]helicenes **10a–h** were deduced from their ^{1}H, ^{13}C, and ^{1}H–^{1}H COSY NMR spectra. Their selected ^{1}H NMR data and chemical shifts are gathered in Tables 3 and 4. For example, protons H_1 and H_{12} for compounds **10a–d** undergo a large deshielding effect compared to the other aromatic protons owing to the magnetic anisotropic effect in the vicinity of the terminal benzene rings, representing the characteristic signals of a [4]helicene [41]. A singlet around $\delta = 8.29, 8.20, 8.26$, and 8.16 ppm is mainly attributed to proton H_6 for compounds **10a**, **10b**, **10c**, and **10d**, respectively. The assignment of the other signals can be determined based on the ^{1}H–^{1}H COSY NMR.
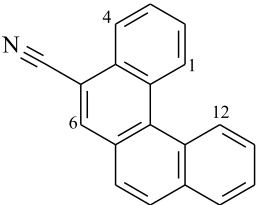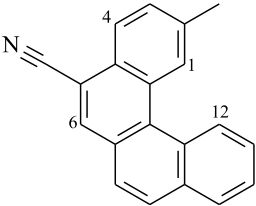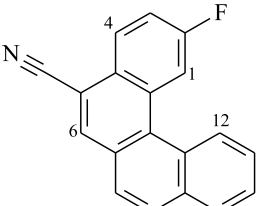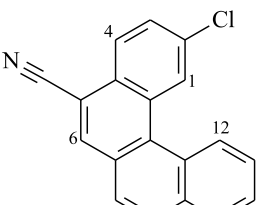
Starting with compound **10b**, the ^{1}H NMR spectrum displayed the characteristic methyl group at 2.68 ppm and eight signals relative to a total of ten aromatic protons. A singlet at 8.90 ppm and a doublet at 9.05 ppm ($J = 9$ Hz) correspond to protons H_1 and H_{12}, respectively. On the ^{1}H–^{1}H COSY NMR spectrum (Figure 3), proton H_{12} shows a cross peak with a proton among three others appearing as a multiplet at 7.71–7.78 ppm. This latter proton shows another cross peak with the signal proton (m, 1H) at 8.03–8.06 ppm. Consequently, H_{11} belongs to the multiplet at 7.71–7.78 ppm and the signal which appears as a multiplet within the range 8.03–8.06 ppm is therefore relative to proton H_{10}. A correlation is observed between the doublet at $\delta = 7.64$ ppm ($J = 8.1$ Hz) and the doublet at $\delta = 8.32$ ppm ($J = 8.1$ Hz), which allows us to assign these two doublets to protons H_3 and H_4, respectively. The difference in NMR chemical shifts between them is closely explained by the effect of substituents at C_2 (Me) and C_5 (CN). H_4 is more deshielded than H_3 owing to the proximity of cyano

group. Also, the doublet at $\delta = 7.92$ ppm ($J = 8.7$ Hz) shows a cross peak with the multiplet (3H) within the range 7.71–7.78 ppm. So, this doublet could be attributed to proton H_7 or H_8 and the multiplet was assigned to protons H_9, H_{11}, and H_7 or H_8.

According to the structure of compound **10c**, it is easy to assign the doublet of doublet at $\delta = 8.68$ ppm ($J_{H-H} = 1.8$ Hz, $J_{H-F} = 11.7$ Hz) to proton H_1 that couples with fluorine and proton H_3. As a proton inside the crown, H_{12} reveals as a doublet with characteristic downfield shifts at $\delta = 8.9$ ppm ($J = 8.1$ Hz). The assignment of the other signals could be elaborated thanks to COSY experiment (Figure 3). For instance, the correlation between the doublet of H_{12} and the multiplet at 7.74–7.82 ppm, which is relative to 3 protons, confirms that one of these protons is H_{11}. That proton (H_{11}) shows a correlation with the signal appearing at 8.06 ppm, which is clearly attributed to proton H_{10}. The multiplet at 7.53–7.60 ppm corresponds to H_3 since it shows two correlations: one with H_1 and a second with the doublet of doublet at 8.42 ppm ($J_{H-H} = 9$ Hz, $J_{H-F} = 6$ Hz) corresponding to H_4. When observing the correlations between the multiplet at 7.74–7.82 ppm and the doublet appearing at $\delta = 7.98$ ppm ($J = 8.4$ Hz), we can assign this last signal to proton H_7 or H_8 and the multiplet to protons H_9, H_{11}, and H_8 or H_7.

Furthermore, the ^{1}H NMR data of compounds **10e–h** show the same characteristics of a [4]helicene: the two most deshielded signals are assigned to protons H_1 and H_{11} which are inside the crown. A singlet and a doublet or doublet of doublet corresponding to protons H_6 and H_8, respectively, are deshielded owing to the electron-withdrawing effect of the nitrile group and also represent characteristic protons of this family of benzo[*b*]naphtho[2,1-*d*]thiophene-7-carbonitrile. As previously, the assignment of the other signals was

Table 3. Selected characteristic ^{1}H NMR (300 MHz) data (δ in ppm) for compounds **10a–d**

Compound	δ (H$_1$)	δ (H$_6$)	δ (H$_4$)	δ (H$_{12}$)
10a	9.11–9.14 (m)	8.44–8.49 (m)	8.29 (s)	9.05–9.08 (m)
10b	8.90 (s)	8.32 (d)	8.20 (s)	9.05 (d)
10c	8.68 (dd)	8.42 (dd)	8.26 (s)	8.9 (d)
10d	8.96 (d)	8.23 (d)	8.16 (s)	8.84 (d)

s, singlet; d, doublet; dd, doublet of doublet; m, multiplet.

based on ^{1}H–^{1}H COSY NMR spectral analysis (Figure 4). In the case of compound **10f**, protons H$_{11}$ and H$_8$ appear as a singlet at δ = 8.72 ppm and a doublet at δ = 8.24 ppm (J = 8.4 Hz), respectively. Each one of them displays a cross peak with the same proton signal belonging to the multiplet (3H) at 7.52–7.65 ppm, which is clearly attributed to H$_9$. We noted a cross peak between the doublet of H$_1$ (δ = 8.77 ppm) and the last multiplet (3H) and a cross peak between the doublet at δ = 7.97 ppm (J = 7.8 Hz) and the same multiplet. These correlations clearly proved that the

multiplet around 7.52–7.65 ppm corresponds to protons H$_2$ and H$_3$, while the doublet at δ = 7.97 ppm is attributed to H$_4$.

Compound **10h** exhibits very similar ^{1}H NMR data to that of **10f** within the range of 7.20–9.00 ppm. Indeed, the doublet at δ = 8.62 ppm (J = 8.4 Hz) and the doublet at δ = 8.83 ppm (J = 1.5 Hz) could be assigned to H$_1$ and H$_{11}$, respectively. The ^{1}H–^{1}H COSY NMR spectrum of **10h** (Figure 4) shows the same four correlations as that of **10f** between H$_1$ and H$_2$, H$_{11}$ and H$_9$, H$_8$ and H$_9$, and H$_4$ and H$_3$. This
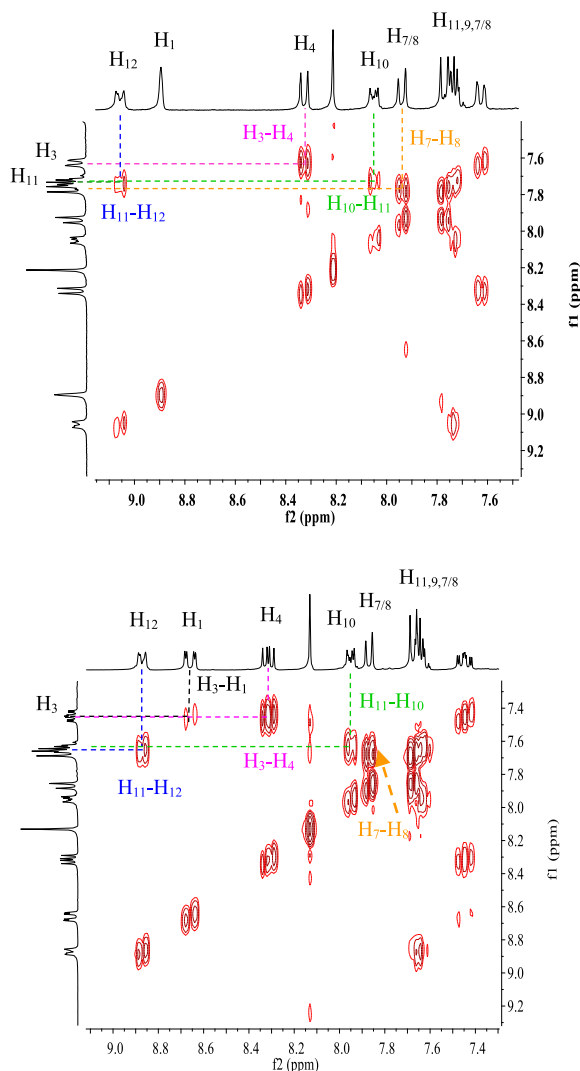
Figure 3. Expansion between 7.4 and 9.2 ppm of ^{1}H–^{1}H COSY NMR spectra (CDCl$_3$, 300 MHz, 298 K) of compounds **10b** (top) and **10c** (down).

allows us to conclude that the multiplet around 7.58–7.67 ppm corresponds to protons H$_2$, H$_3$, and H$_9$.

Photophysical properties of the novel compounds **10a–h** have been performed using UV–Vis absorption and photoluminescence (PL) spectroscopies at room temperature. The absorption spectra were measured in different solvents such as chloroform (CHCl$_3$), methanol (MeOH), tetrahydrofuran (THF), *N*,*N*-dimethylformamide (DMF), and cyclohexane and the resulting optical parameters are gathered in Tables 5 and 6. In dilute chloroform solutions
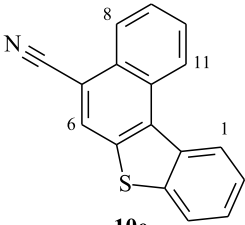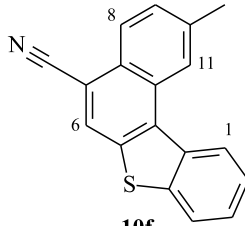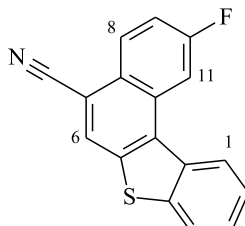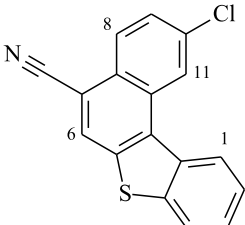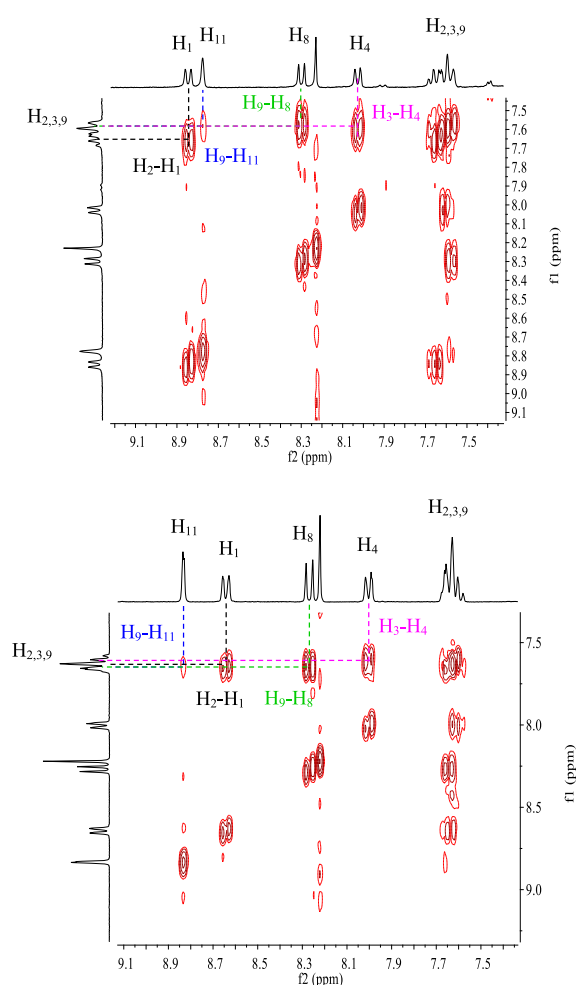

Figure 4. Expansion between 7.4 and 9.1 ppm of ^{1}H–^{1}H COSY NMR spectra (CDCl$_3$, 300 MHz, 298 K) of compounds **10f** (top) and **10h** (down).

($c \approx 1.5 \times 10^{-5}$ mol·L^{-1}), the absorption spectra of compounds **10a–d** exhibited similar features including several bands, with very close absorption coefficients, that are characteristic of π–π* and n–π* transitions (Figure 5). In the high-energy region, two thin and intense absorption bands are observed at 263 nm (ε ~ 132 000–138 000 M^{-1}·cm^{-1}) and 270 nm (ε ~ 128 000–134 000 M^{-1}·cm^{-1}). By examining the low-energy region (300–350 nm), three absorption bands are clearly identified around 315, 328, and 343 nm for compounds **10a**, **10c**, and **10d**, respectively, and a bathochromic shift of about 5 nm was noted for the absorption maxima of **10b**. At longer wavelengths (>350 nm), two weaker absorption

Table 4. Selected characteristic ^{1}H NMR (300 MHz) data (δ in ppm) for compounds **10e–h**

Compound	δ (H$_1$)	δ (H$_6$)	δ (H$_8$)	δ (H$_{11}$)
10e	8.79 (dd)	8.27 (s)	8.38 (dd)	8.96 (d)
10f	8.77 (d)	8.17 (s)	8.24 (d)	8.72 (s)
10g	8.73 (d)	8.30 (s)	8.04 (d)	8.62 (dd)
10h	8.62 (d)	8.22 (s)	8.25 (d)	8.83 (d)

s: singlet, d: doublet, dd: doublet of doublet, m: multiplet.

bands are located between 350 nm and 400 nm with intensities within the range 17 900–24 800 M^{-1}·cm^{-1} revealing a hypsochromic shift of about 3–4 nm for the absorption maxima of **10c**.

The absorption spectra of **10a–d** in the other solvents showed markedly different behaviors especially below 300 nm. In cyclohexane and THF, the tetracyclic systems **10a–d** absorbed strongly within the range 250–300 nm. In THF solutions, their absorption spectra displayed a strong absorption at 279 nm

($\varepsilon \approx 253\,000$ M^{-1}·cm^{-1}) and a shoulder peak located at 298 nm. In MeOH, only a broad band was observed with a maximum peak (111 000–122 000 M^{-1}·cm^{-1}) around 268 nm. By changing CHCl$_3$, MeOH, and THF to cyclohexane, the UV–Vis spectra showed a vibronic absorption. When using DMF, a weak absorption at 296–301 nm could be found.

We noticed a remarkable difference regarding the intensities of the absorption bands for compounds **10a–d** in cyclohexane, methanol, and DMF within

Table 5. UV–Vis absorption properties of **10a–h** in $CHCl_3$, THF, MeOH, and cyclohexane

Compound	CHCl₃			THF		
	λ_{abs}[a] (nm)	λ_{onset} (nm)	$E_{g\text{-op}}$[b] (eV)	λ_{abs}[a] (nm)	λ_{onset} (nm)	$E_{g\text{-op}}$[b] (eV)
10a	232, 263, 269, 315, 328, 343, 371, 391	402	3.08	279, 303, 313, 327, 341, 369, 389	400	3.10
10b	263, 270, 299, 318, 332, 347, 370, 391	401	3.09	279, 303, 314, 328, 342, 367, 387	398	3.11
10c	263, 270, 299, 315, 328, 343, 368, 388	397	3.12	279, 303, 316, 329, 344, 371, 390	397	3.12
10d	263, 270, 299, 318, 331, 346, 372, 392	402	3.08	279, 303, 316, 330, 345, 370, 391	400	3.10
10e	263, 270, 292, 306, 336, 370	389	3.18	279, 303, 325, 340, 354, 372	386	3.21
10f	263, 270, 294, 306, 341, 374	388	3.19	279, 303, 329, 340, 354, 372	387	3.20
10g	263, 270, 292, 306, 336, 370	384	3.22	279, 303, 325, 338, 354, 368	383	3.23
10h	263, 270, 296, 309, 331, 344, 375	390	3.17	279, 311, 329, 343, 355, 374	388	3.19

Compound	MeOH			Cyclohexane		
	λ_{abs}[a] (nm)	λ_{onset} (nm)	$E_{g\text{-op}}$[b] (eV)	λ_{abs}[a] (nm)	λ_{onset} (nm)	$E_{g\text{-op}}$[b] (eV)
10a	235, 268, 313, 326, 340, 370, 389	400	3.10	243, 249, 256, 262, 270, 297, 312, 326, 340, 368, 388	397	3.12
10b	279, 315, 329, 343, 369, 389	403	3.07	243, 249, 256, 262, 270, 299, 316, 328, 343, 369, 388	396	3.13
10c	237, 279, 313, 326, 341, 367, 387	398	3.11	243, 249, 256, 262, 270, 297, 315, 328, 343, 369, 389	397	3.12
10d	242, 279, 316, 327, 342, 370, 389	401	3.09	243, 249, 256, 262, 270, 283 295, 315, 328, 343, 369, 389	398	3.11
10e	235, 263, 290, 301, 324, 338, 372	388	3.19	243, 249, 256, 262, 270, 291 302, 311, 324, 337, 354, 366, 373	383	3.23
10f	235, 266, 281, 291, 327, 340, 371	386	3.21	243, 249, 256, 262, 270, 292 305, 327, 340, 353, 366, 371	382	3.24
10g	233, 245, 266, 291, 307, 323, 337, 368	383	3.23	243, 249, 256, 262, 270, 290 305, 311, 324, 333, 338, 350, 362, 370	378	3.28
10h	236, 268, 294, 310, 327, 341, 373	386	3.21	243, 249, 256, 262, 270, 294 308, 313, 328, 342, 355, 367, 373	383	3.23

[a]Absorption maxima measured in solution ($c \approx 1.5 \times 10^{-5}$ mol·L^{-1}) at room temperature.

[b] The optical gap ($E_{g\text{-op}}$) was estimated from the onset point of the absorption spectrum: $E_{g\text{-op}} = 1240/\lambda_{onset}$.
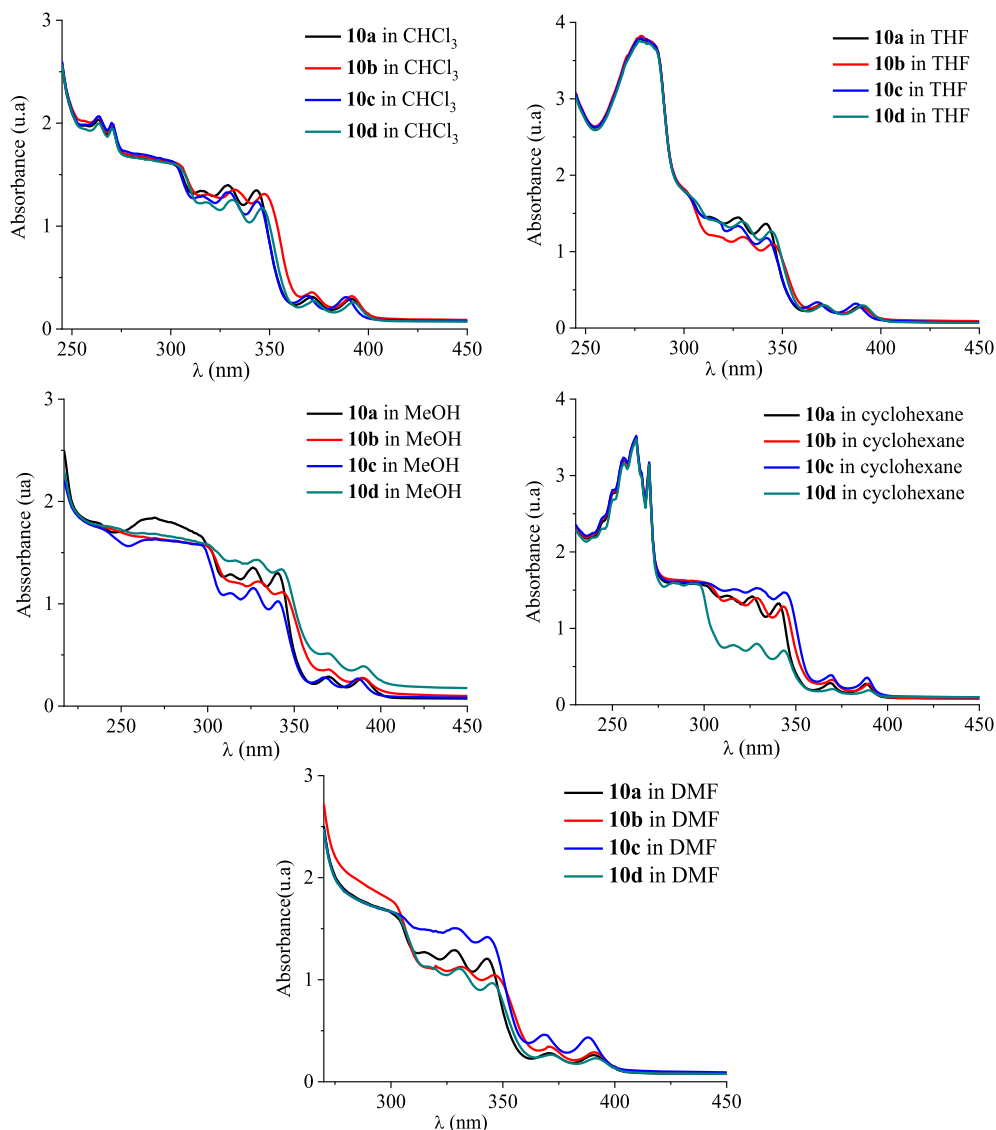
Figure 5. UV–Vis absorption spectra of [4]helicenes **10a–d** in CHCl$_3$, THF, MeOH, cyclohexane, and DMF in dilute solutions ($c \approx 1.5 \times 10^{-5}$ mol·L^{-1}).

the range 300–400 nm. Compared to **10a–c**, compound **10d** exhibited five less intense absorption bands (λ = 316, 328, 343, 369, and 389 nm) in cyclohexane, CHCl$_3$, and DMF, but the most intense ones in MeOH. On the contrary, the intensities of the bands for compound **10c** were found to be the highest in DMF and cyclohexane, but low in MeOH. The other compounds exhibited similar bands with comparable intensities.

As depicted in Figure 6, the absorption spectra

of compounds **10e–h** in CHCl$_3$, THF, MeOH, cyclohexane, and DMF at room temperature exhibit similar features as compounds **10a–d** below 278 nm, but they absorbed differently in the highest wavelengths. In the low-energy region (>300 nm), the absorption spectra of the benzo[*b*]naphto[2,1-*d*]thiophene-7-carbonitriles **10e–h** show several and remarkably larger bands, compared to those of **10a–d**. This resulting behavior may be explained by the elongation of the conjugated structure due to the presence
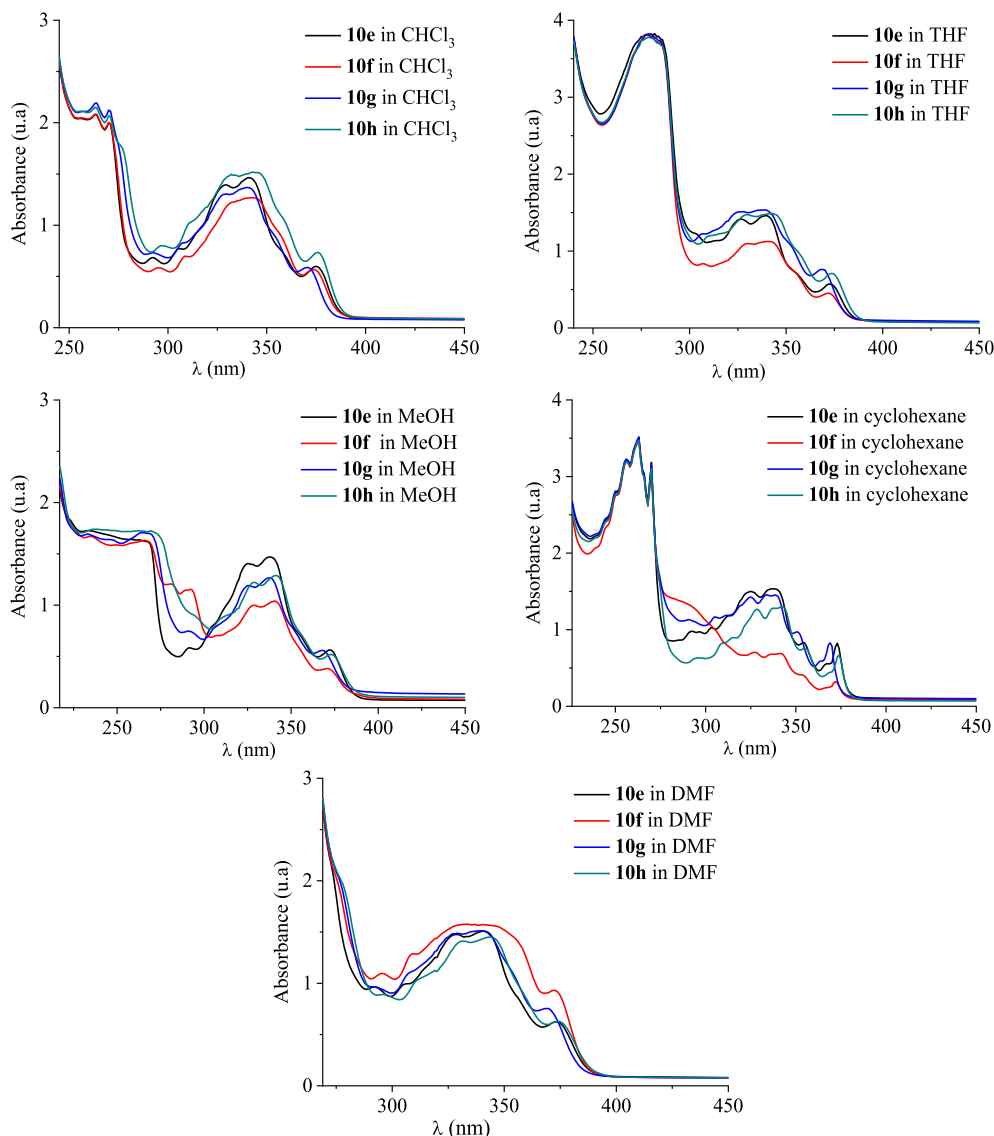
Figure 6. UV–Vis absorption spectra of [4]helicenes **10e–h** in CHCl$_3$, THF, MeOH, cyclohexane, and DMF in dilute solutions ($c \approx 1.5 \times 10^{-5}$ mol·L^{-1}).

of a thiophene nucleus in **10e–f**. It is interesting to notice that compound **10h** shows a bathochromic shift of about 3–4 nm for the low-energy maxima at 374 nm in THF. Moreover, in cyclohexane the low-energy maxima at 373 nm for compounds **10e,h** are slightly shifted to the highest wavelengths.

As shown in Figures 7 and 8, a strong absorbance accompanied by a large bathochromic shift of about 15 nm within the range 250–300 nm is observed in dilute THF solutions. Compounds **10c**, **10f**, **10g**, and **10h** showed less absorption bands when changing the solvent from CHCl$_3$, cyclohexane, DMF, or THF to MeOH. The change of solvent does not considerably affect the photophysical features of compounds **10a**,**e** at longer wavelengths ranging from 320 nm to 400 nm. The absorption bands above 350 nm are less intense than the other observed ones and could be ascribed to the intramolecular charge transfer (ICT) from the [4]helicene unit to the electron-withdrawing cyano group. The optical gap energy
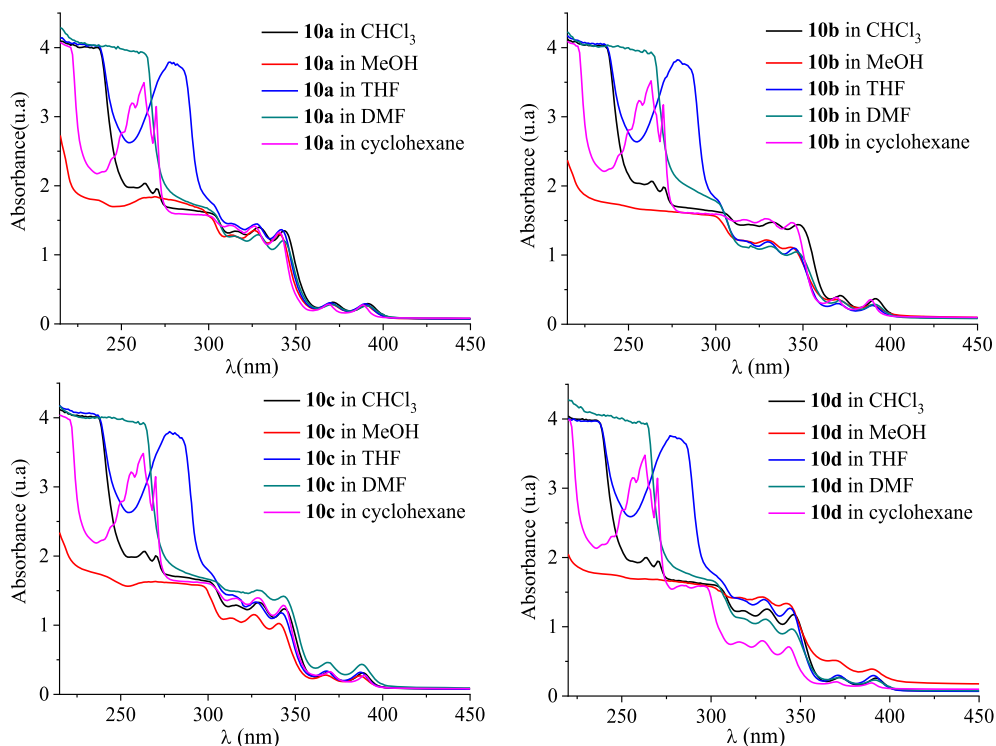
Figure 7. UV–Vis absorption spectra of [4]helicenes **10a–d** in increasing polarity of the tested solvents ($c \approx 1.5 \times 10^{-5}$ mol·L^{-1}) at room temperature.

Table 6. UV–Vis absorption properties of **10a–h** in DMF

Compound	λ_{abs}[a] (nm)	λ_{onset} (nm)	$E_{g\text{-op}}$[b] (eV)
10a	296, 314, 328, 343, 370, 390	403	3.07
10b	299, 320, 331, 346, 370, 390	403	3.07
10c	301, 316, 329, 343, 368, 387	401	3.09
10d	297, 317, 330, 345, 371, 391	403	3.07
10e	292, 304, 326, 341, 373	389	3.18
10f	294, 308, 326, 341, 373	388	3.19
10g	292, 306, 325, 340, 371	386	3.21
10h	296, 312, 329, 344, 374	391	3.17

[a]Absorption maxima measured in solution ($c \approx 1.5 \times 10^{-5}$ mol·L^{-1}) at room temperature.

[b]The optical gap ($E_{g\text{-op}}$) was estimated from the onset point of the absorption spectrum: $E_{g\text{-op}} = 1240/\lambda_{onset}$.

($E_{g\text{-opt}}$) of each [4]helicene was calculated from the absorption onset and was found to be 3.07 to 3.31 eV (Tables 5 and 6). Their UV profiles resembled those of some tetracyclic systems having interesting photophysical properties [42–44].

The photoluminescence (PL) spectra of [4]helicenes **10a–h** have been recorded in chloroform solutions ($c \approx 1.5 \times 10^{-5}$ mol·L^{-1}) at room temperature showing a blue light emission (Figure 9). Compounds **10a–d** present structured emissions displaying two
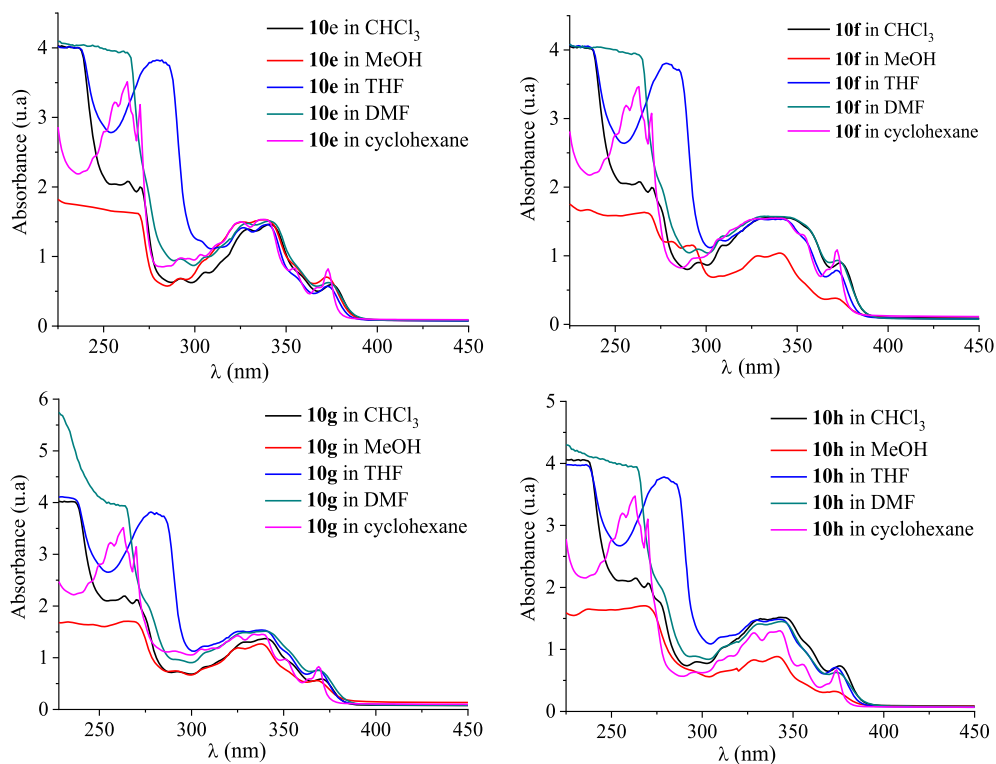
Figure 8. UV–Vis absorption spectra of [4]helicenes **10e–h** in increasing polarity of the tested solvents ($c \approx 1.5 \times 10^{-5}$ mol·L^{-1}) at room temperature.
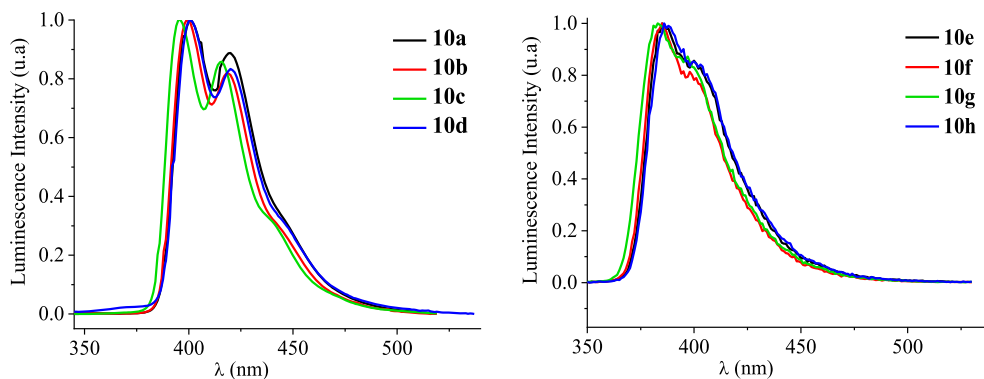

Figure 9. Normalized emission spectra ($\lambda_{exc} = 340$ nm) of **10a–h** in dilute chloroform solutions ($c \approx 1.5 \times 10^{-5}$ mol·L^{-1}).

bands with different intensities followed by one shoulder peak (Table 7). The emission maximum of the fluorinated derivative **10c** ($\lambda_{ems} = 395$ nm) is shifted to the lower wavelengths by 4–5 nm, in comparison to those of **10a,b,d** ($\lambda_{ems} = 399$–400 nm). Unlike the previous compounds, the emission spec-

tra of the benzo[*c*]phenanthrene-like derivatives **10e–h** show one slightly wider main emission band ($\lambda_{ems} = 385$–388 nm) incorporating a shoulder peak around 395 nm.

Table 7. Photoluminescence properties of [4]helicenes **10a–h** in chloroform. Stokes shifts are calculated in wavelength and wavenumber units

Compound	Photoluminescence		Stokes shift	
	λ_{ems}^a (nm)	FWHM^d (nm)	$\lambda_{ems}^{max}-\lambda_{1abs}$ (nm)	$\Delta\nu$ (cm^{-1})
10a	400^b, 419, 441^c	43	9	575
10b	399^b, 419, 438^c	41	8	512
10c	395^b, 415, 435^c	39	7	456
10d	400^b, 420, 440^c	41	8	510
10e	386^b, 395^c	41	16	1120
10f	385^b, 396^c	38	11	763
10g	388^b, 395^c	40	13	917
10h	387^b, 397^c	40	12	826

^{a} Emission measured in chloroform ($c \approx 1.5 \times 10^{-5}$ mol·L^{-1}) at room temperature; fluorescence excitation at 340 nm.

^{b} Emission maximum (λ_{ems}^{max}).

^{c} Shoulder peak.

^{d} Spectrum full width at half maximum.

4. Conclusion

In conclusion, we have achieved the synthesis of various α,β-unsaturated nitriles bearing reactive functional groups, which are precursors of new [4]helicenes. Our synthetic strategy involves only two steps and offers a simple and direct pathway toward a series of functionalized tetracyclic π-conjugated systems in good overall yields. The UV–Vis absorption and the photoluminescence properties of the target benzo[*c*]phenanthrene and benzo[*b*]naphto[2,1-*d*]thiophene derivatives have been experimentally evaluated in solutions and an emission in the blue region of the visible spectrum was noted. The obtained results seem encouraging for the examination of such compounds as promising materials for opto-electronic applications.

Acknowledgments

References

[1] M. S. Newman, W. B. Wheatley, *J. Am. Chem. Soc.*, 1948, **70**, 1913-1916.

[2] R. S. Cahn, C. Ingold, V. Prelog, *Angew. Chem. Int. Ed.*, 1966, **5**, 385-415.

[3] M. S. Newman, R. M. Wise, *J. Am. Chem. Soc.*, 1956, **78**, 450-454.

[4] G. Bringmann, J. Hinrichs, J. Kraus, A. Wuzik, T. Schulz, *J. Org. Chem.*, 2000, **65**, 2517-2527.

[5] M. C. CarreÇo, S. Garcia-Cerrada, M. J. Sanz-Cuesta, A. Urbano, *Chem. Commun.*, 2001, **2001**, 1452-1453.

[6] C. Herse, D. Bas, F. C. Krebs, T. Bürgi, J. Weber, T. Wesolowski, B. W. Laursen, J. Lacour, *Angew. Chem., Int. Ed.*, 2003, **42**, 3162-3166.

[7] K. Hamrouni, N. Hafedh, M. Chmeck, F. Aloui, *J. Mol. Struct.*, 2020, **1217**, article no. 128399.

[8] N. Hafedh, F. Aloui, S. Raouafi, *J. Mol. Struct.*, 2018, **1165**, 126-131.

[9] H. Okubo, M. Yamaguchi, C. Kabuto, *J. Org. Chem.*, 1998, **63**, 9500-9509.

[10] L. Mei, J. M. Veleta, T. L. Gianetti, *J. Am. Chem. Soc.*, 2020, **142**, no. 28, 12056-12061.

[11] W. Shen, S. Graule, J. Crassous, C. Lescop, H. Gornitzka, R. Reau, *Chem. Commun.*, 2008, **2008**, 850-852.

[12] K. Kano, H. Kamo, S. Negi, T. Kitae, R. Takaoka, M. Yamaguchi, H. Okubo, M. Hirama, *J. Chem. Soc., Perkin Trans.*, 1999, **2**, 15-22.

[13] H. Okubo, D. Nakano, S. Anzai, M. Yamaguchi, *J. Org. Chem.*, 2001, **66**, 557-563.

[14] T. R. Kelly, R. A. Silva, H. De Silva, S. Jasmin, Y. Zhao, *J. Am. Chem. Soc.*, 2000, **122**, 6935-6949.

[15] A. Abhervé, K. Martin, A. Hauser, N. Avarvari, *Eur. J. Inorg. Chem.*, 2019, **2019**, 4807-4814.

[16] T. Biet, T. Cauchy, Q. chao Sun, J. Ding, A. Hauser, P. Oulevey, T. Bürgi, D. Jacquemin, N. Vanthuyne, J. Crassous, N. Avarvari, *Chem. Commun.*, 2017, **53**, 9210-9213.

[17] T. Biet, A. Fihey, T. Cauchy, N. Vanthuyne, C. Roussel, J. Crassous, N. Avarvari, *Chem. Eur. J.*, 2013, **19**, 13160-13167.

[18] M. A. Baldo, D. F. OBrien, Y. You, A. Shoustikov, S. Sibley, M. E. Thompson, S. R. Forrest, *Nature*, 1998, **395**, 151-154.

[19] S. Reineke, F. Lindner, G. Schwartz, N. Seidler, K. Walzer, B. Lussem, K. Leo, *Nature*, 2009, **459**, 234-238.

[20] M. Watson, A. Fechtenkotter, K. Müllen, *Chem. Rev.*, 2001, **101**, 1267-1300.

[21] R. G. Harvey, *Curr. Org. Chem.*, 2004, **8**, 303-323.

[22] J. E. Anthony, *Chem. Rev.*, 2006, **106**, 5028-5048.

[23] J. Wu, W. Pisula, K. Müllen, *Chem. Rev*, 2007, **107**, 718-747.

[24] J. Wu, *Curr. Org. Chem.*, 2007, **11**, 1220-1240.

[25] X. Feng, W. Pisula, K. Müllen, *Pure Appl. Chem.*, 2009, **81**, 2203-2224.

[26] H. Zhang, D. Wu, S. H. Liu, J. Yin, *Curr. Org. Chem.*, 2012, **16**, 2124-2158.

[27] J. Mei, Y. Diao, A. L. Appleton, L. Fang, Z. Bao, *J. Am. Chem. Soc.*, 2013, **135**, 6724-6746.

[28] J. E. Anthony, *Angew. Chem., Int. Ed.*, 2008, **47**, 452-483.

[29] T. Hatakeyama, S. Hashimoto, M. Nakamura, *Org. Lett.*, 2011, **13**, 2130-2133.

[30] K. Schickedanz, T. Trageser, M. Bolte, H.-W. Lerner, M. Wagner, *Chem. Commun.*, 2015, **51**, 15808-15810.

[31] C. Shen, E. Anger, M. Srebro, N. Vanthuyne, K. K. Deol, T. D. Jefferson Jr, G. Muller, J. A. G. Williams, L. Toupet, C. Roussel, J. Autschbach, R. Réau, J. Crassous, *Chem. Sci.*, 2014, **5**, 1915-1927.

[32] L. Norel, M. Rudolph, N. Vanthuyne, J. A. G. Williams, C. Lescop, C. Roussel, J. Autschbach, J. Crassous, R. Réau, *Angew. Chem., Int. Ed.*, 2010, **49**, 99-102.

[33] E. Anger, M. Rudolph, L. Norel, S. Zrig, C. Shen, N. Vanthuyne, L. Toupet, J. A. G. Williams, C. Roussel, J. Autschbach, J. Crassous, R. Réau, *Chem. Eur. J.*, 2011, **17**, 14178-14198.

[34] O. Crespo, B. Eguillor, M. A. Esteruelas, I. Fernandez, J. G. Raboso, M. G. Gallego, M. M. Ortiz, M. Olivan, M. A. Sierra, *Chem. Commun.*, 2012, **48**, 5328-5330.

[35] C. Shen, E. Anger, M. Srebro, N. Vanthuyne, L. Toupet, C. Roussel, J. Autschbach, R. Réau, J. Crassous, *Chem. Eur. J.*, 2013, **19**, 16722-16728.

[36] N. Saleh, B. Moore, M. Srebro, N. Vanthuyne, L. Toupet, J. A. G. Williams, C. Roussel, K. K. Deol, G. Muller, J. Autschbach, J. Crassous, *Chem. Eur. J.*, 2015, **21**, 1673-1681.

[37] M. B. Gawande, R. V. Jayaram, *Catal. Commun.*, 2006, **7**, 931-935.

[38] A. Lorente, C. Galan, I. Fonseca, J. Sanz-Aparicio, *Can. J. Chem.*, 1995, **73**, 1546-1555.

[39] F. D. Lewis, D. E. Johnson, *J. Photochem.*, 1977, **7**, 421-423.

[40] C. S. Wood, F. B. Mallory, *J. Org. Chem.*, 1964, **29**, 3373-3377.

[41] K. D. Bartle, D. W. Jones, *Adv. Org. Chem.*, 1972, **8**, 317-423.

[42] J.-Y. Hu, A. Paudel, N. Seto, X. Feng, M. Era, T. Matsumoto, J. Tanaka, M. R. J. Elsegood, C. Redshaw, T. Yamato, *Org. Biomol. Chem.*, 2013, **11**, 2186-2197.

[43] X. Zhang, E. L. Clennan, T. Petek, J. Weber, *Tetrahedron*, 2017, **73**, 508-518.

[44] H. Guédouar, F. Aloui, B. Ben Hassine, *J. Adv. Chem.*, 2016, **22**, 4404-4412.